Available online at www.sciencedirect.com
ScienceDirect
Journal of Fluorine Chemistry 128 (2007) 65–70
JOURNAL OF FLUORINE CHEMISTRY
www.elsevier.com/locate/fluor

Experimental and theoretical studies on inversion dynamics of dichloro(L-difluoromethionine-*N*,*S*)platinum(II) and dichloro(L-trifluoromethionine-*N*,*S*)platinum(II) complexes

Mark D. Vaughan [a], Valerie J. Robertson [b], John F. Honek [a,*]

[a] *Department of Chemistry, University of Waterloo, Waterloo, Ontario N2L 3G1, Canada*
[b] *Department of Chemistry, University of Guelph, Guelph, Ontario N1G 2W1, Canada*

Received 2 August 2006; received in revised form 3 October 2006; accepted 4 October 2006
Available online 13 October 2006

Abstract

Fluorinated analogues of methionine such as L-*S*-(difluoromethyl)homocysteine (L-difluoromethionine; DFM) and L-*S*-(trifluoromethyl)homocysteine (L-trifluoromethionine; TFM) have been demonstrated to be interesting analogues for incorporation into peptides and proteins. The presence of the fluorine nucleus adjacent to the sulfur atom in the side chain not only serves to alter the nucleophilicity and electron density of the sulfur atom but it can function as an important NMR spectroscopic (^{19}F) probe. Additional information on the properties of these fluorinated amino acid analogues was obtained by studying their interactions with dipotassium tetrachloroplatinate (K_2PtCl_4). The resulting complexes, dichloro(L-difluoromethionine-*N*,*S*)platinum(II) and dichloro(L-trifluoromethionine-*N*,*S*)platinum(II) were investigated with respect to their sulfur inversion rates utilizing dynamic NMR methods. Inversion barriers for the DFM– and TFM–platinum complexes were experimentally determined to be 16.4 ± 0.2 and 18 ± 1 kcal/mol, respectively. Density functional calculations at the B3LYP/SDD level were also performed to model the structures and energies of the ground and transition states for these complexes.

Keywords: Difluoromethionine; Trifluoromethionine; Platinum complexes; Dynamic NMR; B3LYP/SDD

1. Introduction

Fluorinated amino acids have recently attracted much attention for their potential in imparting unique physical and chemical characteristics to protein and peptide molecules [1]. Fluorinated amino acids have been shown to dramatically increase thermal stability in a 4-helix bundle protein [2] and leucine zipper coiled coil structures [3,4] and also permit self-sorting of peptides containing these modified residues, which may have implications in the design of protein folding pathways. Incorporation of fluorinated methionine analogues into the chemotactic fMet–Leu–Phe tripeptide enhance the ability of this peptide to attract neutrophils [5]. Additionally, fluorinated amino acids have been utilized extensively in ^{19}F NMR investigations into the structural and dynamic properties of proteins in solution [6–8].

Methionine (Met) residues in proteins are able to coordinate metal centres, often in redox proteins such as cytochrome *c*, where they assist in defining the enzyme redox potential [9]. Thus, it may be possible to alter the catalytic properties of these redox proteins by perturbing the electronic features of the methionine thioether group. We have previously demonstrated that the fluorinated Met analogues L-difluoromethionine (*S*-difluoromethyl-L-homocysteine; L-DFM) and L-trifluoromethionine (*S*-trifluoromethyl-L-homocysteine; L-TFM) can be biosynthetically incorporated into recombinant proteins without diminishing catalytic activity [10–14]. *Ab initio* modeling experiments with these compounds suggest that the strongly electron-withdrawing effect of the fluorine atoms on the methyl group should significantly decrease the nucleophilicity of the sulfur atom, which could alter some aspects of the interaction between this atom and a metal ligand [5].

In order to increase our understanding of the interactions of fluorinated methionine analogues with metal centers, we have chosen the well-known reaction of Met with K_2PtCl_4 as a model system [15–18]. In solution, methionine acts as a bidentate

* Corresponding author. Tel.: +1 519 888 4567; fax: +1 519 746 0435.
E-mail address: jhonek@uwaterloo.ca (J.F. Honek).

0022-1139/$ – see front matter © 2006 Elsevier B.V. All rights reserved.
doi:10.1016/j.jfluchem.2006.10.009

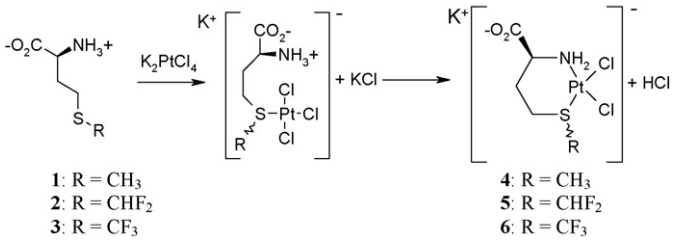

Scheme 1.

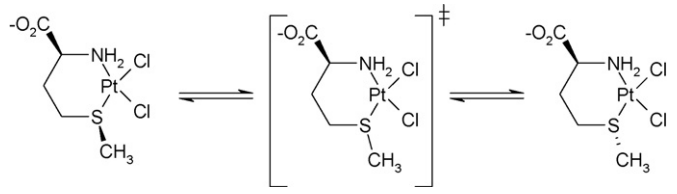

Scheme 2.

chelator of K_2PtCl_4, with initial attack by a lone pair on the sulfur atom, followed by ring closure, as shown in Scheme 1. The resulting cyclic complex exhibits chirality at the sulfur atom, yielding two diastereomeric products. These diastereomers are prone to interconversion through pyramidal inversion at the sulfur atom, similar to that observed for tertiary amines (Scheme 2) [19,20]. The simplicity of the system permits the measurement of reaction rates for formation of the complex by UV–vis spectroscopy and the investigation of changes in the dynamic properties of the complex with increasing fluorination using dynamic nuclear magnetic resonance (NMR) methods. Additionally, changes in structural and bonding features were investigated by *ab initio* computational methods. The results of these studies indicate that fluorination of the methionine methyl group decreases the reactivity of the thioether toward metals but does not contribute to the dynamic properties of the resulting complex.

2. Results and discussion

2.1. Complexation of K_2PtCl_4 by Met analogues

To obtain a preliminary estimate of the reactivity of the various methionine analogues, initial rates for their reaction with K_2PtCl_4 were determined by UV–vis spectroscopy, monitoring the disappearance of the absorbance at 390 nm arising from K_2PtCl_4 (Table 1). These results indicated a decrease in the reaction rate with increasing fluorination, which is likely attributable to the decreasing nucleophilicity of the sulfur atom [5] although it should be noted that the trifluoromethyl moiety is thought to be similar in size to an isopropyl group [21]. A comparison of the reactivities of TFM compared to 2-amino-4-(isopropylthio)butanoic acid towards K_2PtCl_4 would aid in analyzing the extent of the contribution of steric versus electronic factors to the reduced reactivity of TFM. Another analogue of methionine, selenomethionine **7**, was found to be more reactive with K_2PtCl_4 than Met, DFM and TFM, which may be due in part to its larger and more diffuse electron shell [22]. Ethionine **8** was also investigated and its observed rate was quite similar to that of Met. The very low reaction rate observed for norleucine **9**, which lacks a chalcogen in the side chain, supports the suggestion that the decrease in absorbance during the course of the reaction is primarily attributable to formation of the Pt–S bond with minimal contributions from Pt–N coordination.

Table 1
Reaction rates for coordination of K_2PtCl_4 by various methionine analogues

Amino acid	Rate (mM s^{-1})
L-Selenomethionine (**7**)	129 ± 4
L-Methionine (**1**)	32 ± 2
L-Ethionine (**8**)	26.1 ± 0.9
L-Difluoromethionine (**2**)	0.50 ± 0.02
L-Trifluoromethionine (**3**)	0.18 ± 0.04
L-Norleucine (**9**)	0.053 ± 0.001
Control	0.021 ± 0.001

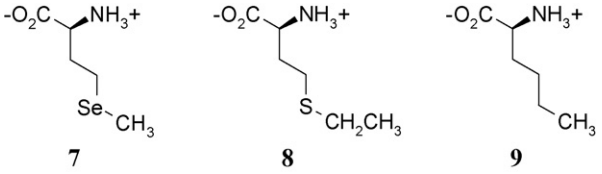

2.2. Sulfur inversion rates for DFM– and TFM–platinum complexes

Because the sulfur atom possesses two lone pairs available for coordination, two products result from the reaction of Met with K_2PtCl_4 which differ in the stereochemistry at the sulfur position [17]. These two diastereomers are in dynamic equilibrium via a thermally controlled inversion of the sulfur configuration [19,20,23]. The temperature dependence for the rate of this interconversion between stereoisomers in the Met, DFM, and TFM complexes was determined by NMR spectroscopy using lineshape analysis [24,25]. A plot of inversion rate

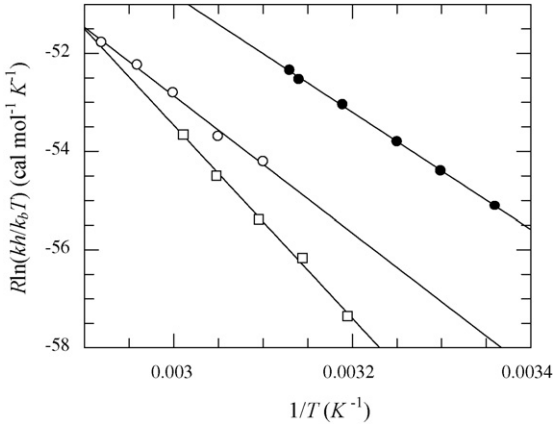

Fig. 1. Eyring plot for sulfur inversion in complexes **4**–**6**: (○) complex **4**, (●) complex **5**, (□) complex **6**. Thermodynamic parameters obtained from this plot are given in Table 2.

versus temperature yields a sigmoidal curve, as the spectra become insensitive to exchange rates at temperatures significantly higher or lower than the coalescence temperture (data not shown). This rate information was used to create Eyring plots for these three complexes, shown in Fig. 1 (because the inversion is a zero-order kinetic process, the rate and rate constant are equal). From these curves, the enthalpy ($\Delta^{\ddagger}H^{\circ}$) and entropy ($\Delta^{\ddagger}S^{\circ}$) of activation for this inversion in each complex was determined. These parameters were then used to obtain $\Delta^{\ddagger}G^{\circ}$ for each process (Table 2).

Unlike the observed reaction rates for complex formation, there is no direct correlation between the number of fluorine atoms present on the methyl position and the inversion rate. The three coordination compounds show very similar results, with the activation barriers observed for the Met, DFM and TFM complexes being 17 ± 1, 16.4 ± 0.2 and 18 ± 1 kcal/mol, respectively. These results suggest that steric and electronic effects associated with Met fluorination have surprisingly little net effect on the inversion parameters in the cyclic complex.

The barrier for sulfur inversion in *N*-acetyl-Met·$PtCl_3$ has previously been evaluated at 15.9 kcal/mol (at 335 K) [20]. This value is in good agreement with the results obtained herein, the ~1 kcal/mol difference within the error associated with these experiments. As an interesting note, the value obtained for *N*-acetyl-Met·$PtCl_3$ was determined by ^{195}Pt NMR using the temperature coalescence method. This result lends support to our findings as the two experiments show good agreement despite the use of different experimental methods. A survey of the available literature accounts detailing the thermodynamics of sulfur inversion in various platinum(II)-thioether compounds reveals that the inversion barrier typically falls between 15 and 20 kcal/mol [23,26–29], an observation which is supported by our results.

In theory, the entropy of activation for a process which does not involve bond scission or formation should be near zero, as the overall order of the system remains relatively unchanged throughout the process [26]. The values for $\Delta^{\ddagger}S^{\circ}$ observed in this experiment deviate significantly from zero; however, previous studies have shown that the error in $\Delta^{\ddagger}S^{\circ}$ determined by dynamic NMR methods is often quite large [30–32] and can be solvent-dependent as well [33].

2.3. Computational studies

To develop a better understanding of the molecular changes possibly induced in the Met·$PtCl_2$ complex by fluorination, *ab initio* geometry optimizations at the B3LYP/SDD level were performed on the ground state *R* and *S* structures of compounds **4–6** (note: *R* and *S* are used throughout to denote configurations at the sulfur atom. In all cases, the stereochemistry at the amino acid C_α is exclusively *S*). Initial coordinates were obtained from the crystal structure of **4** [17], and the corresponding fluorinated compounds were constructed by replacement of the appropriate number of protons with fluorine atoms. The optimized ground state geometries were then utilized to model a transition state for the inversion using the quadratic synchronous transit approach. Energy calculations for the ground states and transition states permitted the calculation of the activation barriers for $R \rightarrow S$ and $S \rightarrow R$ inversion in each complex, summarized in Table 2.

Calculated Pt–S bond lengths are quite similar in the ground state structures of the three complexes, with a decrease in bond length of 0.01–0.02 Å with increasing fluorination. Crystallographic structures of compounds **10** and **11** [34,35] show the opposite trend, the bis-trifluoromethylated compound incorporating longer Pt–S bonds as indicated, which might suggest inadequacies in the ability of the B3LYP/SDD computational level to model the fluorinated Met complexes.

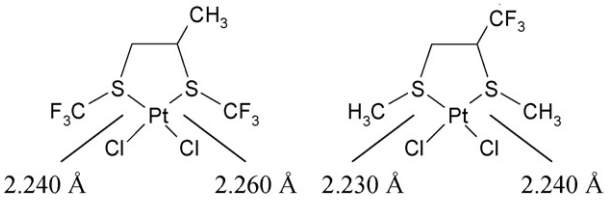

10 **11**

Transition state structures for sulfur inversion (Fig. 2) were modelled using the quadratic synchronous transit approach [36,37], with an initial guess for the transition state generated manually by placing the methyl group coplanar with the platinum coordination plane. The results of these calculations predict that the inversion barriers in the three complexes should be quite similar (Table 2). Structurally, the calculated transition state conformations for the three compounds are very similar overall, with the ring assuming a half-chair conformation and the C_ε–S–Pt–N dihedral angles deviating only 1–3° from planarity.

The trend in the computational results agrees well with that observed experimentally, with the calculated free energies of inversion showing no significant sensitivity to the degree of fluorination. However, these calculated values underestimate the experimental values by 3–5 kcal/mol. Moreover, the calculated ground state structure of the non-fluorinated

Table 2
Experimentally and computationally[a] determined thermochemical parameters for sulfur inversion in compounds **4–6**

Compound	$\Delta^{\ddagger}H^{\circ}_{exp}$ (kcal/mol)	$\Delta^{\ddagger}S^{\circ}_{exp}$ (cal/mol K)	$\Delta^{\ddagger}G^{\circ}_{exp}$ (kcal/mol)	$\Delta^{\ddagger}G^{\circ}_{calc}$ ($R \rightarrow S$) (kcal/mol)	$\Delta^{\ddagger}G^{\circ}_{calc}$ ($S \rightarrow R$) (kcal/mol)
4	14.0 ± 0.7	11 ± 2	17 ± 1	13.70	13.50
5	11.9 ± 0.1	-15.0 ± 0.5	16.4 ± 0.2	13.26	14.44
6	19.7 ± 0.7	5 ± 2	18 ± 1	13.12	14.36

[a] Data were obtained using Gaussian 98, revision A.9, with geometry optimizations and frequency calculations performed at the B3LYP/SDD level.

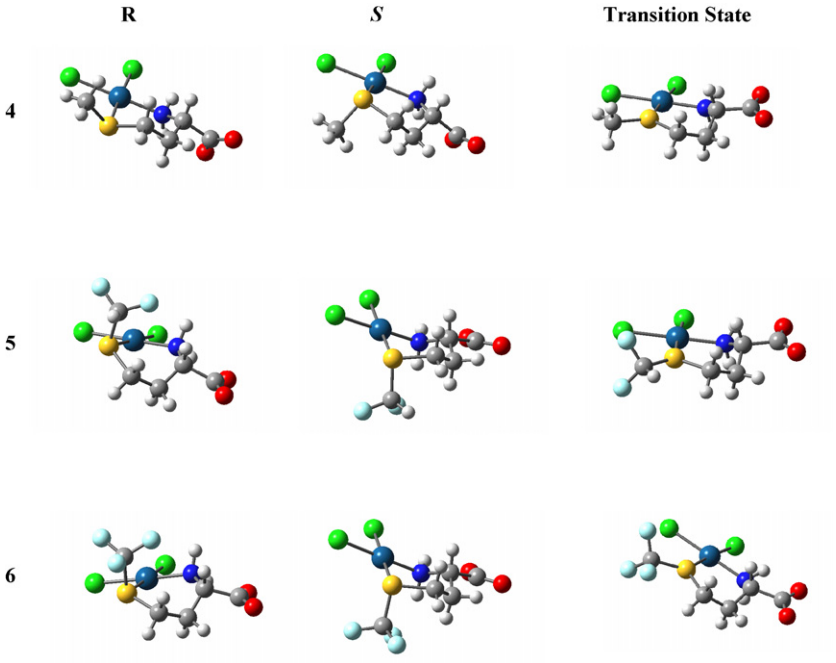

Fig. 2. B3LYP/SDD optimized geometries for *R*, *S*, and transition state structures of complexes **4**–**6**.

methionine complex was found to deviate significantly from the reported crystallographic structure. Taken together, these results illustrate that the B3LYP/SDD computational level is subject to significant limitations in handling platinum-containing compounds [38].

3. Conclusions

Fluorination substantially decreases the reactivity of methionine toward K_2PtCl_4, yet does not have substantive effects on the dynamic properties of the resulting cyclic complex. This is consistent with density functional calculations at the B3LYP/SDD level. These results may have important implications in the design of metalloproteins with altered chemical properties, particularly with regard to the structure of the metal-binding site.

4. Experimental

4.1. General experimental procedures

K_2PtCl_4 (99.9%) was purchased from Alfa Aesar (Ward Hill, MA). L-Methionine, L-selenomethionine, L-ethionine, and L-norleucine were obtained from Sigma (St. Louis, MO) and were of the highest purity available. L-Difluoromethionine and L-trifluoromethionine were prepared as previously described [10,12,39]. All other chemicals were reagent grade and used without further purification. FT-IR spectra were recorded on a Perkin-Elmer Spectrum RX I FT-IR spectrophotometer. Samples were prepared as KBr pellets. Data are expressed in wavenumbers (cm^{-1}). High resolution mass spectra were acquired using a Kratos Concept 1S double focusing mass spectrometer with FAB ionization and negative ion detection. Masses reported represent the major isotopic species (containing ^{195}Pt and ^{35}Cl). The remaining isotopic distribution pattern was as expected based on the natural abundance of each Pt and Cl isotope (Pt isotopic distribution: ^{194}Pt 32.9%, ^{195}Pt 33.8%, ^{196}Pt 25.3%, ^{198}Pt 7.21%; Cl distribution: ^{35}Cl 75.5%, ^{37}Cl 24.5%) [40].

4.1.1. NMR spectroscopy

The 300 MHz ^1H and 282.2 MHz ^{19}F spectra were recorded on a Bruker Avance 300 spectrometer with a 5 mm quadrupole nucleus probe (QNP). The 400 MHz ^1H and 376.3 MHz ^{19}F NMR spectra were recorded using a Bruker Avance spectrometer fitted with a 5 mm inverse broadband probehead. For 376.3 MHz ^{19}F measurements, the proton coil was tuned to fluorine. Standard undecoupled 376.3 MHz ^{19}F parameters were 18,832 Hz sweep width, 0.877 s acquisition time, and a 1.0 s relaxation delay. A 3 Hz line broadening was applied. ^{19}F Spectra were referenced to an external sample of $CFCl_3$ in methanol-d_4 and ^1H spectra to tetramethylsilane (TMS), each set to 0.00 ppm. All samples were prepared in D_2O or 1N HCl in D_2O.

Conformational exchange rates for inversion of sulfur configuration in the Met and DFM complexes were determined by acquiring 400 MHz ^1H NMR spectra at various temperatures. The signals for the methyl and difluoromethyl protons at various temperatures (25–70 °C for Met, 20–50 °C for DFM, 5 °C intervals) were simulated using MEX lineshape simulation software [24] and exchange rates were obtained from the simulated spectral parameters. For an example of a typical experimental spectrum and corresponding simulated spectrum, please refer to Fig. S1 in the supplementary information.

TFM exchange rates were evaluated using selective inversion-recovery in the 376.3 MHz ^{19}F NMR spectrum at various temperatures (40–60 °C, 5 °C intervals), with data analysis performed using the CIFIT program [25]. In this experiment, one of the two ^{19}F resonances arising from the two

sulfur configurations is irradiated with a 180° x′ pulse. Following a time interval τ, the system is irradiated with a 90° $_{x'}$ pulse for detection. When $\tau = 0$, the spectrum consists of two resonances of equal intensity and opposite orientation, the resonance irradiated with the 180° $_{x'}$ pulse appearing as a negative signal. During the delay time τ, the intensities of the two signals are altered due to T_1 relaxation and chemical exchange. An initial guess for the T_1 of each signal can be obtained using a non-selective inversion-recovery by formulating an estimate for the exchange rate and using the CIFIT program to generate a hypothetical T_1 value. These T_1's are then used to fit the data for the selective inversion recovery experiment to generate a better guess for the exchange rate. This new rate is then used for a second round of fitting of the non-selective inversion recovery data to generate improved T_1's. This process is repeated iteratively until a consistent value is obtained for the exchange rate. Spectra from a typical experiment are shown in Fig. S2 and experimental and calculated magnetization for these spectra are shown in Fig. S3 in the supplementary information. For additional detail regarding this approach, please refer to the CIFIT manual, available on the web [41]. Rates for sulfur inversion for complexes **4–6** at various temperatures are presented in Table S1 in the supplementary information.

4.1.2. Synthesis of methionine–platinum complexes

*4.1.2.1. Dichloro(L-methionine-N,S)platinum(II) (**4**).* Methionine–platinum complexes were prepared according to the method of McAuliffe [16]. L-Methionine (46 mg, 0.308 mmol) was added to a stirred solution of potassium tetrachloroplatinate(II) (145 mg, 0.35 mmol) in 0.8 ml distilled, deionized water. This solution was heated to 40 °C for 30 min, during which time a copious yellow precipitate formed. After cooling to 0 °C, the precipitate was isolated by centrifugation, washed with cold water (3× 1 ml), and dried *in vacuo*. To protect the compound from photolytic degradation, manipulations were performed under low lighting whenever possible. Yield was quantitative (139 mg). mp (uncorrected): 219–220 °C (dec.), darkens at 214 °C (lit. mp: 230 °C (darkens) [16]); ^{1}H NMR (300 MHz, 1N HCl in D_2O): δ 2.41 (s, CH_3, epimer *a*), δ 2.39 (s, CH_3, epimer *b*), integration ratio ~1:1; IR (KBr): 3257, 3164, 3100, 2896, 1709, 1572, 1436, 1250, 1101, 975 cm^{-1}; HRMS (FAB): exact mass calculated for $C_5H_{10}Cl_2NO_2Pt$: 413.94572, found 413.95117 (M^-, ^{195}Pt, ^{35}Cl).

*4.1.2.2. Dichloro(L-difluoromethionine-N,S)platinum(II) (**5**).* Compound **5** was prepared similarly to **4** using L-difluoromethionine (57 mg, 0.308 mmol) in place of L-Met, giving 131 mg (87%) of a yellow solid. mp: 208–209 °C (dec.); ^{1}H NMR (400 MHz, 1N HCl in D_2O) δ 7.32 (t, J_{HF} = 53.77 Hz, epimer *a*) δ 7.28 (t, J_{HF} = 53.85 Hz, epimer *b*) ^{19}F NMR (282.2 MHz, 1N HCl in D_2O, ^{1}H decoupled): δ −97.8 (m, J_{FF} = 196 Hz, J_{PtF} = 74.1 Hz, CHF_2, epimer *a*); −97.1 (m, J_{FF} = 196 Hz, J_{PtF} = 61.4 Hz, CHF_2, epimer *b*), integration ratio ~1:1; HRMS (FAB): exact mass calculated for $C_5H_8Cl_2F_2NO_2Pt$: 449.92686, found 449.91491 (M^-, ^{195}Pt, ^{35}Cl).

*4.1.2.3. Dichloro(L-trifluoromethionine-N,S)platinum(II) (**6**).* L-Trifluoromethionine (61 mg, 0.300 mmol) was added to a stirred solution of potassium tetrachloroplatinate(II) (145 mg in 0.8 ml 0.1N aqueous HCl) and heated to 80 °C for 30 min. The product was isolated as described for **4**, yielding 113 mg (72%) of a yellow solid. mp: 200–201 °C (dec.), shrinks at 134 °C. ^{19}F NMR (282.2 MHz, 1N HCl in D_2O): δ −46.6 (pseudo-triplet, J_{PtF} = 69.2 Hz, CF_3, epimer *a*); −46.2 (pseudo-triplet, J_{PtF} = 65.7 Hz, CF_3, epimer *b*), integration ratio ~1:1; IR (KBr) 3196, 2934, 1731, 1582, 1431, 1166, 1094, 754 cm^{-1}; HRMS (FAB): exact mass calculated for $C_5H_7Cl_2F_3NO_2Pt$: 467.91744, found 467.91790 (M^-, ^{195}Pt, ^{35}Cl).

4.1.3. Measurement of K_2PtCl_4–methionine reaction rates

To obtain an estimate of the initial rates for the complexation of K_2PtCl_4 by the series of methionine analogues (Table 1) equimolar quantities of K_2PtCl_4 and the appropriate analogue (5 mM each in 1 ml 50 mM potassium phosphate buffer, pH 7.0, containing 0.2 M KCl) were combined and the decrease in absorbance at 390 nm was monitored using a Varian Cary3 UV–vis spectrophotometer. The linear regions of the resulting curves (i.e. the region over which the absorbance changed by <5% relative to the initial absorbance) were fitted by linear regression analysis (Grafit 3.01, Erithacus Software Ltd.), and the slopes were converted to approximate reaction rates of mM s^{-1} (ε_{390} for K_2PtCl_4 was experimentally determined to be 5.56×10^{-4} M^{-1} cm^{-1}). All kinetic analyses were carried out at 25 ± 0.5 °C.

4.1.4. Computational details

Calculations were performed using Gaussian 98W, Revision A.9 (Gaussian Inc. Pittsburgh, PA) [42]. Computational parameters are expressed using standard notations. Methionine complex geometries were optimized by RHF/LANL2DZ *ab initio* calculations starting with the crystal structures for **4** reported by Freeman and Golomb [17]. These structures were further optimized using the hybrid density functional theory (DFT)/Hartree–Fock functional B3LYP [43] and the SDD basis set, which uses the Dunning/Huzinaga full double zeta basis set on the first-row elements and Stuttgart/Dresden effective core potentials (ECPs) on the remaining elements [44,45]. For each optimized structure, a frequency calculation was also performed using these parameters. Zero point energies calculated from these frequency calculations were used to correct free energy values obtained for each structure. No negative frequencies were found for ground state structures. Transition structures were determined using the quadratic synchronous transit approach, with an initial guess for the transition state generated by adjusting the C_ε–S–Pt–N torsion angle such that the methyl group was coplanar with the platinum plane. The identity of the resulting structure as a transition state was confirmed by the presence of a single negative frequency. Animation of this negative frequency in GaussView (Gaussian Inc., Pittsburgh, PA) verified that the transition corresponded to sulfur inversion and linked the two ground state structures.

Acknowledgements

We thank Dr. A. Bain (McMaster University) for providing the MEX and CIFIT software. Mass spectral analysis was performed by Mr. Tim Jones (Brock University). Financial support by NSERC of Canada and the University of Waterloo (J.F.H.) is gratefully acknowledged. M.D.V. was supported by an NSERC postgraduate scholarship and an Ontario graduate scholarship.

Appendix A. Supplementary data

Supplementary data associated with this article can be found, in the online version, at doi:10.1016/j.jfluchem.2006.10.009.

References

[1] N.C. Yoder, K. Kumar, Chem. Soc. Rev. 31 (2002) 335–341.
[2] H.Y. Lee, K.H. Lee, H.M. Al-Hashimi, E.N. Marsh, J. Am. Chem. Soc. 128 (2006) 337–343.
[3] B. Bilgicer, A. Fichera, K. Kumar, J. Am. Chem. Soc. 123 (2001) 4393–4399.
[4] S. Son, I.C. Tanrikulu, D.A. Tirrell, ChemBioChem 7 (2006) 1251–1257.
[5] M.E. Houston, L. Harvath, J.F. Honek, Bioorg. Med. Chem. Lett. 7 (1997) 3007–3012.
[6] C. Frieden, S.D. Hoeltzli, J.G. Bann, Method Enzymol. 380 (2004) 400–415.
[7] B. Salopek-Sondi, L.A. Luck, Protein Eng. 15 (2002) 855–859.
[8] P.G. Gettins, Int. J. Biol. Macromol. 16 (1994) 227–235.
[9] M. Ubbink, A.P. Campos, M. Teixeira, N.I. Hunt, H.A.O. Hill, G.W. Canters, Biochemistry 33 (1994) 10051–10059.
[10] H. Duewel, E. Daub, V. Robinson, J.F. Honek, Biochemistry 36 (1997) 3404–3416.
[11] H.S. Duewel, E. Daub, V. Robinson, J.F. Honek, Biochemistry 40 (2001) 13167–13176.
[12] M.D. Vaughan, P. Cleve, V. Robinson, H.S. Duewel, J.F. Honek, J. Am. Chem. Soc. 121 (1999) 8475–8478.
[13] B. Salopek-Sondi, M.D. Vaughan, M.C. Skeels, J.F. Honek, L.A. Luck, J. Biomol. Struct. Dynam. 21 (2003) 235–246.
[14] P. Walasek, J.F. Honek, BMC Biochem. 6 (2005) 21.
[15] L.M. Volshtein, M.F. Mogilevkina, Zh. Neorg. Khim. 8 (1963) 597–603.
[16] C.A. McAuliffe, J. Chem. Soc. A (1967) 641–642.
[17] H. Freeman, M.L. Golomb, J. Chem. Soc. D 22 (1970) 1523–1524.
[18] T.G. Appleton, J.W. Connor, J.R. Hall, Inorg. Chem. 27 (1988) 130–137.
[19] D.D. Gummin, E.M.A. Ratilla, N.M. Kostic, Inorg. Chem. 25 (1986) 2429–2433.
[20] J.A. Galbraith, K.A. Menzel, E.M.A. Ratilla, N.M. Kostic, Inorg. Chem. 26 (1987) 2073–2078.
[21] D. O'Hagan, H.S. Rzepa, J. Chem. Soc., Chem. Commun. (1997) 645–652.
[22] F.A. Cotton, Advanced Inorganic Chemistry, 6th ed., Wiley, New York, 1999.
[23] E.W. Abel, S.K. Bhargava, K.G. Orrell, Prog. Inorg. Chem. 32 (1984) 1–118.
[24] A.D. Bain, G.J. Duns, Can. J. Chem. 74 (1996) 819–824.
[25] A.D. Bain, J.A. Cramer, J. Magn. Reson. 118A (1996) 21–27.
[26] M. Oki, in: H. Ohtaki, H. Yamatera (Eds.), Structure and Dynamics of Solutions, Elsevier, Amsterdam, 1992.
[27] S. Toyota, Y. Yamada, M. Kaneyoshi, M. Oki, Bull. Chem. Soc. Jpn. 62 (1989) 1509–1512.
[28] P. Haake, P.C. Turley, J. Am. Chem. Soc. 89 (1967) 4617–4621.
[29] P. Haake, P.C. Turley, J. Am. Chem. Soc. 89 (1967) 4611–4616.
[30] S. Toyota, M. Oki, Bull. Chem. Soc. Jpn. 68 (1995) 1345–1351.
[31] M. Oki, Applications of Dynamic NMR Spectroscopy to Organic Chemistry, VCH Publishers, Deerfield Beach, FL, 1985.
[32] M.I. Rodriguez-Franco, I. Dorronsoro, A. Castro, A. Martinez, Tetrahedron 56 (2000) 1739–1743.
[33] M. Gromova, C.G. Beguin, R. Goumont, N. Faucher, M. Tordeux, F. Terrier, Magn. Reson. Chem. 38 (2000) 655–661.
[34] L. Manojlovic-Muir, K.W. Muir, T. Solomon, Inorg. Chim. Acta 22 (1977) 69–74.
[35] M.N. Hunter, K.W. Muir, D.W.A. Sharp, Acta Crystallogr. C 41 (1985) 1750–1752.
[36] C. Peng, H.B. Ayala, H.B. Schlegel, M.J. Frisch, J. Comp. Chem. 17 (1996) 49–56.
[37] C. Peng, H.B. Schlegel, Israel J. Chem. 33 (1994) 449–454.
[38] Y. Zhang, Z. Guo, X.-Z. You, J. Am. Chem. Soc. 123 (2001) 9378–9387.
[39] M.E. Houston Jr., J.F. Honek, J. Chem. Soc., Chem. Commun. (1989) 761–762.
[40] A.J. Gordon, R.A. Ford, The Chemist's Companion, Wiley, 1972.
[41] A.D. Bain, see http://www.chemistry.mcmaster.ca/faculty/bain/cifman.pdf.
[42] M.J. Frisch, G.W. Trucks, H.B. Schlegel, G.E. Scuseria, M.A. Robb, J.R. Cheeseman, V.G. Zakrzewski, J.A. Montgomery Jr., R.E. Stratmann, J.C. Burant, S. Dapprich, J.M. Millam, A.D. Daniels, K.N. Kudin, M.C. Strain, O. Farkas, J. Tomasi, V. Barone, M. Cossi, R. Cammi, B. Mennucci, C. Pomelli, C. Adamo, S. Clifford, J. Ochterski, G.A. Petersson, P.Y. Ayala, Q. Cui, K. Morokuma, D.K. Malick, A.D. Rabuck, K. Raghavachari, J.B. Foresman, J. Cioslowski, J.V. Ortiz, A.G. Baboul, B.B. Stefanov, G. Liu, A. Liashenko, P. Piskorz, I. Komaromi, R. Gomperts, R.L. Martin, D.J. Fox, T. Keith, M.A. Al-Laham, C.Y. Peng, A. Nanayakkara, M. Challacombe, P.M.W. Gill, B. Johnson, W. Chen, M.W. Wong, J.L. Andres, C. Gonzalez, M. Head-Gordon, E.S. Replogle, J.A. Pople, Gaussian 98, A.9 ed., Gaussian Inc., Pittsburgh, 1998.
[43] A.D. Becke, J. Chem. Phys. 98 (1993) 5648–5652.
[44] L.v. Szentpaly, P. Fuentealba, H. Preuss, H. Stoll, Chem. Phys. Lett. 93 (1982) 555–559.
[45] P. Fuentealba, H. Preuss, H. Stoll, L.v. Szentpaly, Chem. Phys. Lett. 89 (1982) 418–422.